Biomaterials Science

ROYAL SOCIETY OF CHEMISTRY

PAPER

Ve Art cle O h a
Ve Jour al

Cite this: DOI: 10.1039/d1bm00157d

Nano-enabled coordination platform of bismuth nitrate and cisplatin prodrug potentiates cancer chemoradiotherapy *via* DNA damage enhancement†

Yin-Chu Ma, ‡[a] Xin-Feng Tang,‡[b] You-Cui Xu,[b] Wei Jiang,[a] Yong-Jie Xin,[a] Wei Zhao,[a] Xu He,[a] Li-Gong Lu *[a] and Mei-Xiao Zhan*[a]

The combination of chemotherapy and radiotherapy (chemoradiotherapy) is a promising strategy, extensively studied and applied clinically. Meanwhile, radiosensitizers play an important role in improving clinical radiotherapy therapeutic efficacy. There are still some disadvantages in practical applications, because radiosensitizers and drugs are difficult to deliver spatio-temporally to tumor sites and work simultaneously with low efficiency for DNA damage and repair inhibition, leading to an inferior synergistic effect. Herein, a suitable radiosensitizer of nano-enabled coordination platform (NP@PVP) with bismuth nitrate and cisplatin prodrug is developed by a simple synthetic route to improve the effectiveness of chemo-radiation synergistic therapy. When NP@PVP is internalized by a tumor cell, the bismuth in NP@PVP can sensitize radiation therapy (RT) by increasing the amount of reactive oxygen species generation to enhance DNA damage after X-ray radiation; meanwhile, the cisplatin in NP@PVP can inhibit DNA damage repair with spatio-temporal synchronization. NP@PVP is demonstrated to exhibit higher sensitization enhancement ratio (SER) of 2.29 and excellent tumor ablation capability upon irradiation *in vivo* in comparison with cisplatin (SER of 1.78). Our strategy demonstrates that the RT sensitization effect of bismuth and cisplatin based NP@PVP has great anticancer potential in chemo-radiation synergistic therapy, which is promising for clinical application.

Received 28th January 2021,
Accepted 12th March 2021

DOI: 10.1039/d1bm00157d

rsc.li/biomaterials-science

Introduction

Ra a a (RT) a a L a , Lca c c ca , a 50% Lca c a c a a .[1–4] RT ca ff c ca c c ff c a c ff c b aL .[11] b DNA b a , b L a P a ba a - c a LDNA ca c c a c a a , c a c a a c ,[12] a- ff c .[5–7] I a , L c RT a ,[13] WS_2,[14] TaO ,[15] a a c ,[16] a b ab ff c a a c a ba a a a ,[17–22] c a ac fficac .[8–10] M a , a ca a b RT a c b -Z a . A , b ca c b ca L - c ab L ba a a a a a ac a a X-a . T c , a a b ca b RT a b c a ff . H - ffic c a - a a Iac L RT fficac , a a ff c a L a c ab L X-a , b ac a X-a a c ffic , c a a a L a L L ff c a . F , c a a a , b L c a a b c a b . I c (. . c a b . bc a) a a a b a c ca L a a a a .[28] H , ca , ff c .

*ffi 519000, 1987 126. 1969 230027,

†E c c a L a (ESI) a a ab . S DOI: 10.1039/1b 00157

‡T a c b a .

c a a c ca b ac b a , a a , a ca -ba c - a a a ac a ca a ff c . c a . . a c , a a , c a a a a c a ffic L a .[29–31] I a c - . acc . a a c - a - a a a DNA a a . a fficac . H , a c aL RT b a , b . c ff c- c - a a ac ca a ca : a L a . I a , b . L a . a ffic a - a . b . ba a a a a a a , RT ca , a . a . ffic c b - b c b L a a L - DNA a a a , . . c a . . T L , c a L a H , a . ab a c a - a a a c b . A a . , a . . L a a - ab c a a . a fficac LRT a L (NP@PVP) b . a c a . ff c a a c b ff c L c - a a . c a ac . c a .[32] a X- a a a . A Sc 1a, NP@PVP C a , a a . a a c ca . cc c c . c b c a . . (. . -[P . a , . ab b c b RT ac (NH3)2C 2(OOCCH2CH2COOH)2], HOOC–P –COOH), B (NO3)3, ff c . a . P a . . a . 80% L a (PVP) , a Iac . c ca a a , acc . L 50% L a a - b . a c a ac c a a ca c . . c ca , c a L - ac . NP@PVP c . b . a c a Lca ca c a .[33–36] I - . a a ac a a a c a L . a . . , b . c . T b . NP@PVP ca RT c ca a . c ac . c (ROS; b c a . a . LROS . a a c DNA . . ·OH) b ac a .[37–40] A Ia , c b - a a aL X- a a a ; a , c a a L c a a a a , c a NP@PVP ca ca DNA a a a b DNA a a ac - a a , a b a a a L a c a a - a . T b a L ca c a . a a a a a . I c L NP@PVP c . a a c . acc . a a

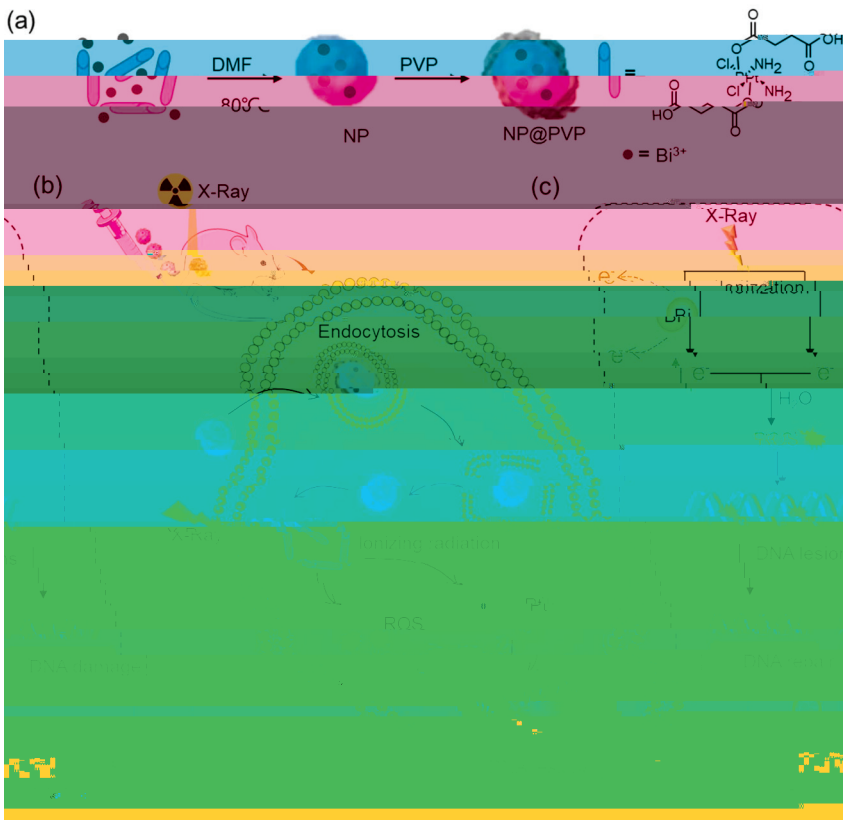

Scheme 1 Schematic representation for (a) the facile synthesis of nano-enabled coordination platform (NP@PVP) with bismuth and cisplatin prodrug and (b, c) the mechanism of enhanced chemo-radiotherapy efficacy under X-ray irradiation.

Experimental

ROS **NP@PVP**

EMT-6 c (b a ca c c , 10^5 c) 24- a (G a J B -F a C . L) a c L 12 . T c c ba c a c a NP@PVP a a P L2 μ L^{-1}. AL 6 , c a a X- a (5 G) a c ba DCFH-DA (10 μM) L a 20 . T c L aL a a a DAPI (b a). ROS (a) a c a c L ca a ca c c (N HD25).

In vivo

A a a c L acc a c G L Ca a U L Lab a A a L U L Sc c a T c L C a (USTC) a a b A a E c C L USTC (A a E ca a W Ia N b : USTCACUC1901022). T -b a c 3 L ac 100 ^{3}. T c L a c PBS, c a , a NP@PVP a a L2 $^{-1}$ P . AL 12 , L L c L ac c X- a a L5 G . T a b a a L ca 3 a a ca c a b L - a ca ab , c a c DNA a a b a c a DNA a ca b a L ROS, a b a a ca c a L c - a a - c a (Sc 1b a c).

Results and discussion

NP@PVP a c c b ac c b ESI.† A a c c c (TEM) a , NP@PVP b a - a - c . T a c a L NP@PVP a a a c ca (DLS), c a ab 190 a F . 1a. F , X- a - c c c (XPS) a a a a c a c ca a c L NP@PVP. A F . 1b, XPS c c L c L B a P NP@PVP. X- a c- c (EDS) a a c L NP@PVP. T EDS a a a a L B a P a 40.11% a 22.78%, c (F . 1c). T a LB a P NP@PVP a a b c c a a a c- . T ca a a L ab 2 : 1 (B : P), c a EDS . H - TEM a (F . 1) a NP@PVP a a L c a a c L L 0.33 a 0.20 , c a (012) a L b a B a a

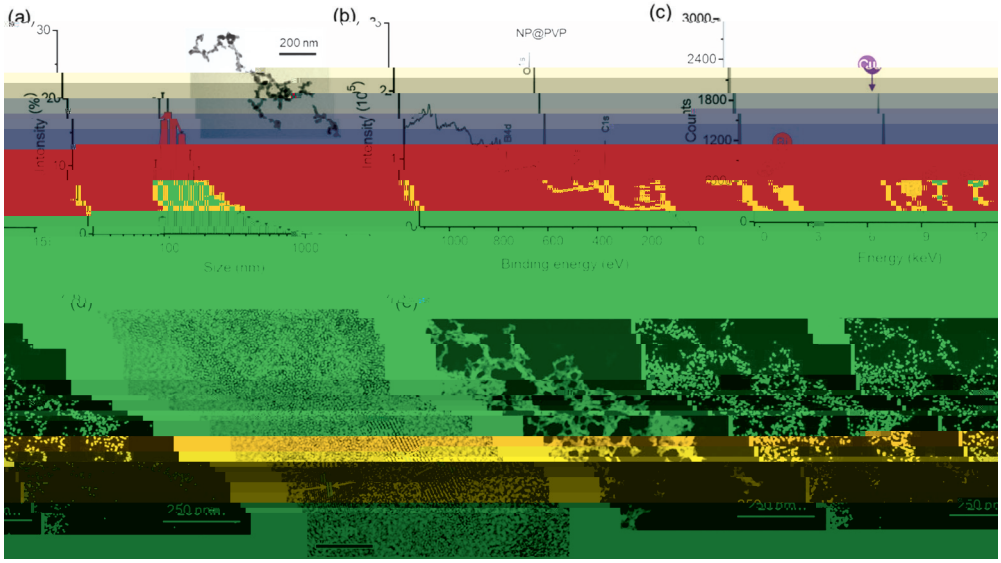

Fig. 1 Synthesis strategy and structural characterization of NP@PVP. (a) Hydrodynamic diameter measured by DLS and corresponding TEM image of NP@PVP. (b) XPS spectrum of NP@PVP. (c) EDS analysis of NP@PVP. (d) High-resolution TEM image of NP@PVP. (e) HAADF-STEM image and EDS element scanning maps of NP@PVP.

(023) a Lc a B_2O_3, c . T c c- L NP@PVP a L b a a a a a a a L ca a - c c c (HAADF-STEM) (F . 1), L c a c a a B a P b - NP@PVP.

T a c a a a L NP@PVP, L C 5- a NP@PVP, a NP@PVP/C 5, c a LNP@PVP EMT-6 b a ca c

L P a NP@PVP, ca P a NP@PVP b ca a a L ROS. I , c - a c RT, c a L c c a a a c aL RT. F , ROS c a NP@PVP a RT c a b 1.89-L a 3.21-L c a c (PBS) a a P a RT, a b -ba NP@PVP a ab X- a a ca ab c a c L a L a ca ROS aL RT. W L a a DNA b - a b a aL c a RT b L c ab L - – 2AX (γ-H2AX) L c .[38] T EMT-6 c a- a b X- a a a L5 G aL b a c - a NP@PVP (c c a LP a 2 μ L^{-1}) L 6 , a c ba L a 0, 1, 4, 12, a 24 L γ-H2AX L c a . A F . 3c a S1,† c a a RT-c a , a acc a L γ

b c c L a , X- a a a L 2, 4, c . H , L c , a , a c a a 8 G c a , , Lc a . A L a ac a , L c c a 12 aL X- a c a , , a Lac L c a NP@PVP/C 5 c , a b EPR ff c L NP@PVP c a c a c a NP@PVP (F . 4c a S3†). c a a . F a c , c , a Lac - F , aL 12 c L NP@PVP c a , a NP@PVP c a 57.8%, 79.4%, 90.2%, a c a a a a X- a (5 G) 96.1% aL c , 2, 4, 6, a 8 G X- a a a . a DCFH–DA (5 , $^{-1}$) a . . c L a M a , c , ca c a a 20 . T ROS , a (, a) a c b a c a a a L c a a NP@PVP , , CLSM. A F . 4 a , , a 1.78 a 2.29, c . NP@PVP + RT L c c , a W , X , IVIS L a a , a (DCF), c a , a a L , a a ac c a b * b LNP@PVP . . T c a + RT a NP@PVP. T ca a a ac c . a a c b a , EMT-6 b , a c a ba NP@PVP c , ff c - , a , (. .) c L NP@PVP/C 5 RT b c a , a , L ROS , a (F . 4a a b). T b a a L b a , a c DNA a a aL X- a a a . . L c a a , - c L E c , a b , L a c L RT - NP@PVP/C 5 a c L , c c a a L C 5 a ff c Lb , NP@PVP . . , L , a c . AL NP@PVP/C 5 c , C 5 c a a ca c a L c - a a c c a , c a a 0.59% L c- a , NP@PVP. T c b a , EMT-6 a 24 . T , acc , a L NP@PVP/C 5 6 , a a c ff a - a c b X , IVIS L a . T PBS (I), PBS + RT (II), c a (III), c a + RT a , L C 5 L , c c , c a aL L C 5 (IV), NP@PVP (V), NP@PVP + RT (VI) (2 , $^{-1}$ LP a 5

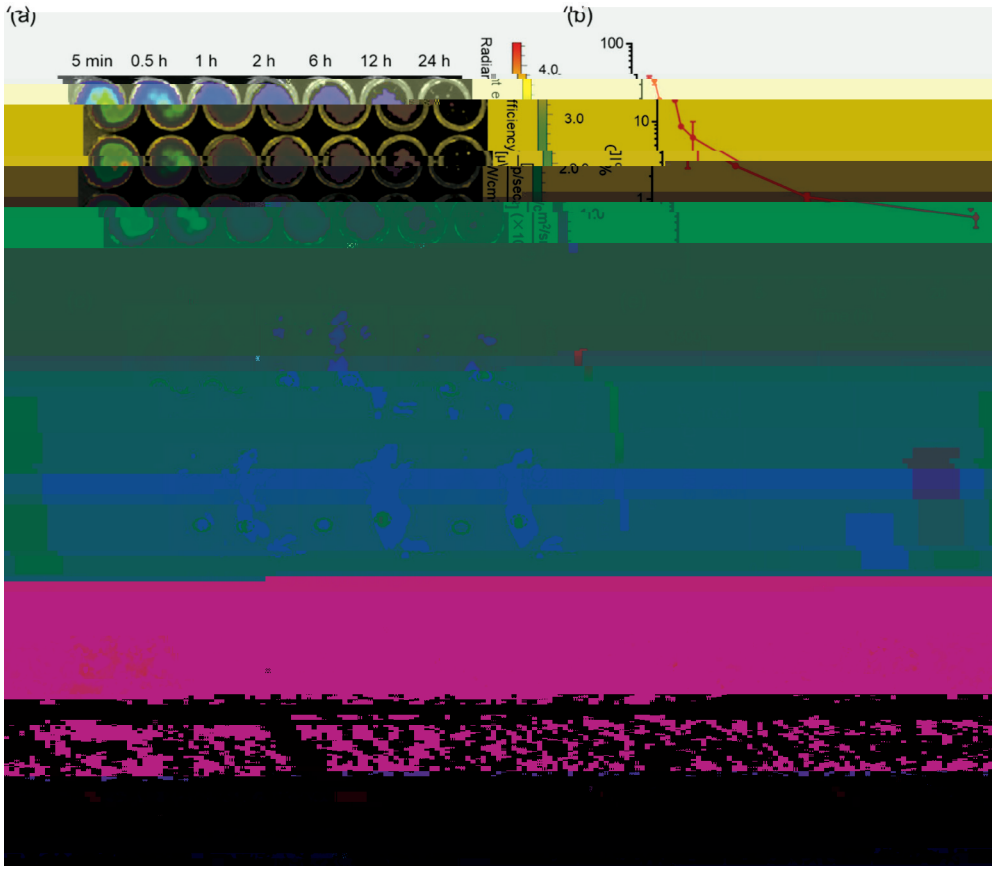

Fig. 4 Biodistribution and tumor accumulation of NP@PVP *in vivo*. (a) Fluorescence images of serum after intravenous (i.v.) injection of NP@PVP/Cy5. (b) Blood circulation curve of NP@PVP/Cy5 after i.v. injection (n = 3 per group). (c) Fluorescence images of mice after i.v. injection of Cy5 or NP@PVP/Cy5. (d) Images of ROS generation *in vivo*. (e) Corresponding DCF fluorescence intensity of tumors after being treated with PBS, NP@PVP, cisplatin + RT and NP@PVP + RT. The error bars represent the means ± SD. $^{**}P < 0.01$, $^{***}P < 0.001$.

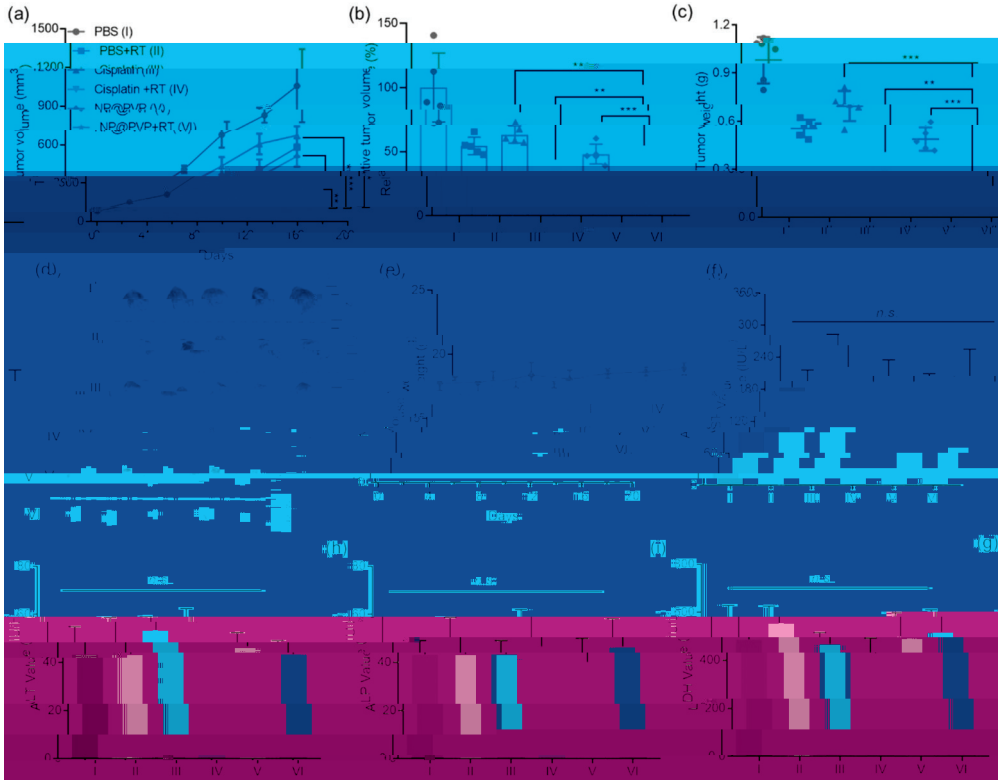

Fig. 5 Excellent tumor inhibition of NP@PVP *in vivo*. (a) Tumor growth changes of mice and (b) tumor inhibition ratio with various treatments of PBS (I), PBS + RT (II), cisplatin (III), cisplatin + RT (IV), NP@PVP (V), and NP@PVP + RT (VI). Tumor weight (c) and pictures of the tumors (d) after treatments. (e) Mice body weights during the antitumor therapy period. The value of aspartate aminotransferase (AST; f), alanine aminotransferase (ALT; g), alkaline phosphatase (ALP; h), and lactate dehydrogenase (LDH; i) in mice after antitumor treatment. Data are shown as the mean ± SD (n = 5), $^{**}P < 0.01$, $^{***}P < 0.001$.

G LX- a a a). T c a Ia PBS (I), c a a a c . T L c b L c - a L c a (III) a NP@PVP (V), a b 36.5% a 51.9% ffic c , c . W c c PBS + RT (II) X- a a a L5 G , 45.4% - b . T L c c c a + RT (IV) a b b 75.9%, c - a a a . A c , a ca c ff c a b c a NP@PVP + RT (91.2% b , VI) ca a L a c L RT a ff c Lb ba NP@PVP a a a - ca c a Lc - a a a . Acc ab , a NP@PVP + RT Lca b , b NP@PVP - RT b c a a L ROS a a c DNA a a aL X- a a a ; a , c a NP@PVP ca ca DNA a a a b DNA a a a a - a c a . A La a , c c L - a a (F . 5a a b). A F . 5c a , a L L a NP@PVP + RT (VI) a ffic c L . T a fficac L ff a L a b H&E a (F . S4†). W c a (III)- NP@PVP (V)- a c a a , c aff c aL b a NP@PVP + RT (VI). T L c a a , c Lca c a aL a b - aL (F . 5). T b L c a c c a a L , c a a ff c L L c aL ff a L c . A F . 5L- , a. L a a a a L a (AST), a a a - a L a (ALT), a a a a (ALP), a ac a a (LDH) L c L c a, a b c a aL a , ca aL .[41] T a a NP@PVP + RT a c ab ff c L c , aL L c - a a .

Conclusions

I a , a cc L c b a a a a - ab c a a L ba b a c a ff c L

c - a a , c a . T b NP@PVP ca RT b c a , a LROS, a a c DNA a a aL X- a a a ; a , c a NP@PVP ca ca DNA a a b DNA a a a c a a - a . I a , c a NP@PVP c b a RT a ca c ff c . Ta , c a a a a L a c L RT a ff c Lb a c a NP@PVP a a a L a ca c c - a a c a , c a L c ca a ca .

Conflicts of interest

T a c L c L ca .

Acknowledgements

T b G a Ba c a A Ba c R ac F a (2020A1515111059), Na a K R ac a D P a L C a (2017YFA0205200), C a P c a Sc c F a (2019TQ0399 a 2020M673044), a F a a R ac F L C a U (WK2070000160).

Notes and references

1 G. E -A baba, L. A. Ca a , T. Ta , M. Z , H. A baba, P. J. Ob , E. A. C cca, R. W , A. G. Ka a c a B. A. Ta , , 2019, **13**, 4028–4040.
2 E. C. K a S. C. F , ., 2019, **95**, 936–939.
3 C. G a b , S. G. E , M. Q. W , F. K. K a a J. S. L ffl , ., 2019, **16**, 729–745.
4 X. J. C , Y. Y , Y. H. Da , X. S , G. Ya , Y. Pa a C. C. G , , 2017, **7**, 4087–4098.
5 T. H a , E. P a , C. L , B. H a R. A. S a a, , 2008, **8**, 193–204.
6 S. G , D. N a W. Ca , , 2017, **11**, 5233–5237.
7 L. W , L. C , S. Z , J. Z , G. D a , Y. Wa , G. Wa , Z. C a , Z. L a M. Ga , ., 2016, **28**, 5072–5079.
8 X. D , R. C , S. Z , H. L , R. Z , C. Z a , ., A c c W$_{2.9}$-WS$_2$ a a - c a ca ab a a c c b c a a a a , , 2020, **14**, 5400–5416.
9 F. Ma , L. W , C. S , S. Z a , G. Wa , J. Z , ., U a a b c a b B$_2$S$_3$ a L a a - c a a a a ca c , , 2016, **10**, 11145–11155.
10 D. H , S. L , C. Z a , J. H , Z. Z , H. Z a a Y. H , , 2017, **11**, 10159–10174.
11 D. L , A. J , X. Wa , H. L , B. O. E , S. S , J. L , G. Ra a , C. A. F a a C. B a, ., 2020, **20**, 7159–7167.
12 W. Fa , B. S , W. B , F. C , K. Z a , S. Z a , L. Z , W. P , Q. X a a H. X , ., 2013, **135**, 6494–6503.
13 Y. Y , C. Z a , Z. G , J. D , Z. G , X. D , J. X , G. Z a , X. L a Y. Z a , , 2017, **11**, 7164–7176.
14 Y. Y , X. C , T. Ba , M. Z , L. Ya , W. Y , C. G , D. Wa , Z. G a Y. Z a , , 2015, **9**, 12451–12463.
15 G. S. S , Y. Y. C , C. L a , X. Y , J. J. L , X. Q. S , S. D. S , K. Ya a Z. L , ., 2016, **28**, 7143.
16 X. D. Z a , Z. L , J. C , X. S , S. S , Y. S , S. Fa , F. Fa , D. T. L a J. X , ., 2014, **26**, 4565–4568.
17 G. S , C. L a , X. Y , Q. Z a , L. C , K. Ya a Z. L , ., 2016, **28**, 2716–2723.
18 J. M. K a, R. E. J , P. P. Ka a , A. M. R , V. R. K a a , N. C. G a c , E. R a , D. S. ac a M. J. Sa , ., 2011, **50**, 12308–12311.
19 H. H a , L. Z. H , W. H. Z , G. B. Q , J. H. Wa , N. Ya , J. Ga , T. F. C , P. K. C a X. F. Y , , 2018, **171**, 12–22.
20 M. Ma, Y. H a , H. R. C , X. Q. J a, S. G. Wa , Z. Z. Wa a J. L. S , , 2015, **37**, 447–455.
21 N. Y , Z. J. Wa , J. L. Z a , Z. X. L , B. Z , J. Y , M. F. Z , C. P a Z. G. C , , 2018, **161**, 279–291.
22 X. J. Y , A. L , C. Z. Z a , K. Ya , X. Y. C a W. W. L , , 2017, **11**, 3990–4001.
23 A. A Za , D. J , Z. L. C , A. L. B. D Ba , G. Ka , J. D a A. T a , , 2014, **8**, 104–112.
24 K. L. A , Y. L. L , J. H. L , Q. H. Y a , Y. Y. H a L. H. L , ., 2011, **23**, 4886–4891.
25 S. Ba a , J. C a , H. K a baba , M. H - G a Ia , T. J. W b a L. Ta b , , 2020, **9**, 1901695.
26 R. Z , H. Wa , Y. Ya , C. Z a , X. D , J. D , L. Ya , G. Z a , Z. G a Y. Z a , , 2019, **189**, 11–22.
27 J. L , X. P. Z , L. Ya , L. J. Z , G. T a , W. Y. Y , L. M. Wa , Y. L , Z. B. H , Z. J. G , C. Y. C a Y. L. Z a , , 2015, **9**, 696–707.
28 J. M. K a, R. E. J , P. P. Ka a , A. M. R , V. R. K a a , N. C. G a c , E. R a , D. S. ac a M. J. Sa , ., 2011, **50**, 12308–12311.
29 L. D , D. S , M. L , L. Ya , H. Ra , P. L , X. Ca , Y. S a Z. Wa , , 2020, **8**, 858–870.
30 Y. Z , D. J. FL , P. A a L. Sa c , ., 2008, **169**, 481–482.

31 L. H a , Z. J. L , Y. Z a , Y. W. Z a , S. W , J. Z. Z a a G. Ha , , 2016, **138**, 14586–14591.

32 Y. D , Y. G , X. L , X. L , S. Wa , L. Wa , G. L , X. Z a , H. Wa , X. G a J. C a , , 2016, **10**, 2536–2548.

33 R. G. K a C. J. Ma , , 2019, **119**, 1058–1137.

34 R. a M , E. S , Y. S , F. K , W. J. M. M a T. La , , 2019, **14**, 1007–1017.

35 T. C. J , K. S a a a a S. J. L a , , 2016, **116**, 3436–3486.

36 X. Y. Wa , X. H. Wa a Z. J. G , , 2015, **48**, 2622–2631.

37 W. J a , Q. L , Z. C. Z , Q. Wa , J. X. D , Y. M. Z a , W. F. L , F. Z , Y. D. Ya , G. Q. Z a , H. L , Y. C. Wa a J. Wa , , 2018, **10**, 35734–35744.

38 S. J. K , J. H. H , C. Pa , H. J. K , G. S. O , J. N. L , S. J. Y , S. K. C , H. S. S , D. J. L , S. K. M a R. Pa , 2015, **47**, 142.

39 W. J a , Q. L , L. X a , J. X. D , Y. L , W. H. Y , Y. C. Ma, X. Q. L , Y. Z. Y , Z. T. T , H. L , H. L a , L. G. L , X. D. X , Y. D. Ya , G. Q. Z a , Y. C. Wa a J. Wa , , 2018, **12**, 5684–5698.

40 P. A. Ma, H. H. X a , C. Y , J. H. L , Z. Y. C , H. Q. S , X. Y. Z a , C. X. L , J. Q. Wa , Z. G a J. L , , 2017, **17**, 928–937.

41 Y. Ma, Y. Z a , N. K. B a , X. Ta , W. J a , J. D , M. I. K a , Q. Wa , J. X a a H. L , , 2019, **13**, 8890–8902.